

# MANUFACTURED SOLUTIONS FOR AN ELECTROMAGNETIC SLOT MODEL

Brian A. Freno

Neil R. Matula

Robert A. Pfeiffer

Evelyn A. Dohme

Joseph D. Kotulski

Sandia National Laboratories

16th World Congress on Computational Mechanics  
4th Pan American Congress on Computational Mechanics  
July 21–26, 2024

Sandia National Laboratories is a multimission laboratory managed and operated by National Technology and Engineering Solutions of Sandia, LLC., a wholly owned subsidiary of Honeywell International, Inc., for the U.S. Department of Energy's National Nuclear Security Administration under contract DE-NA-0003525.

# Outline

- Introduction
- Governing Equations
- Code-Verification Approaches
- Numerical Examples
- Summary

## Outline

- Introduction
    - Electromagnetic Integral Equations
    - Verification and Validation
    - Error Sources
    - This Work
  - Governing Equations
  - Code-Verification Approaches
  - Numerical Examples
  - Summary

## Electromagnetic Integral Equations

- Are commonly used to model electromagnetic scattering and radiation
  - Relate surface current to incident electric and/or magnetic field
  - Discretize surface of electromagnetic scatterer with elements
  - Evaluate 4D reaction integrals over 2D test and source elements
  - Contain singular integrands when test and source elements are near

# Electromagnetic Aperture and Slot Models

- EM penetration occurs through openings of otherwise enclosed surfaces
  - Penetration may occur intentionally or unintentionally
  - Slot connects exterior surface of scatterer to interior surface of cavity
  - Model slot as wires carrying magnetic current located at apertures
    - Exterior surface interacts with exterior wire
    - Interior surface interacts with interior wire
    - Exterior and interior wires interact with each other
    - Exterior and interior surfaces do not interact directly

## Verification and Validation

Credibility of computational physics codes requires verification and validation

- **Validation** assesses how well models represent physical phenomena
    - Compare computational results with experimental results
    - Assess suitability of models, model error, and bounds of validity
  - **Verification** assesses accuracy of numerical solutions against expectations
    - *Solution verification* estimates numerical error for particular solution
    - *Code verification* verifies correctness of numerical-method implementation

## Code Verification

- Code verification most rigorously assesses rate at which error decreases
  - Error requires exact solution – usually unavailable
  - Manufactured solutions are popular alternative
    - Manufacture an arbitrary solution
    - Insert manufactured solution into governing equations to get residual term
    - Add residual term to equations to coerce solution to manufactured solution
  - For integral equations, few instances of code verification exist
  - Analytical differentiation is straightforward – analytical integration is not
  - Numerical integration is necessary, generally incurs an approximation error
  - Therefore, manufactured source term may have its own numerical error

## Error Sources in the Electromagnetic Integral Equations

### 3 sources of numerical error:

- **Domain discretization:** Representation of curved surfaces with planar elements
    - Second-order error for curved surfaces, no error for planar surfaces
    - Error reduced with curved elements
  - **Solution discretization:** Representation of solution or operators
    - Common in solution to differential, integral, and integro-differential equations
    - Finite number of basis functions to approximate solution
    - Finite samples queried to approximate underlying equation operators
  - **Numerical integration:** Quadrature
    - Analytical integration is not always possible
    - For well-behaved integrands,
      - Expect integration error at least same order as solution-discretization error
      - Less rigorously, error should decrease with more quadrature points
    - For (nearly) singular integrands, **monotonic convergence is not assured**

# This Work

## Isolate solution-discretization error

- Manufacture solution
- Eliminate numerical-integration error by manufacturing Green's function
- Mitigate contamination from discontinuity due to wire–surface interaction

## Isolate numerical-integration error

- Manufacture solution
- Cancel solution-discretization error using basis functions

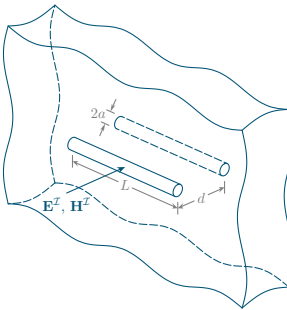
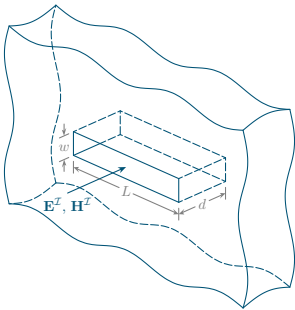
## Avoid domain-discretization error

- Consider only planar surfaces
- Previously provided approaches to account for domain-discretization error

# Outline

- Introduction
- Governing Equations
  - Overview
  - The Electric-Field Integral Equation
  - The Slot Equation
  - Discretization
- Code-Verification Approaches
- Numerical Examples
- Summary

# Thick Slot Model Overview



- Electromagnetic scatterer encloses a cavity
- Exterior is connected to interior by rectangularly prismatic slot with  $L \gg w, d$  (left)
- Slot is replaced with two thin wires at apertures that carry magnetic current (right)
- Exterior and interior surfaces interact with wires, not each other
- Wires interact with each other – magnetic current is equal and opposite
- EFIE solved on each surface, slot equation solved for wires

# The Electric-Field Integral Equation

In time-harmonic form,  $\mathbf{E}^S$  computed from  $\mathbf{J}$  and  $\mathbf{M}$

Scattered electric field       $\mathbf{E}^S(\mathbf{x}) = -\left(j\omega \mathbf{A}(\mathbf{x}) + \nabla \Phi(\mathbf{x}) + \frac{1}{\epsilon} \nabla \times \mathbf{F}(\mathbf{x})\right)$

Magnetic vector potential       $\mathbf{A}(\mathbf{x}) = \mu \int_{S'} \mathbf{J}(\mathbf{x}') G(\mathbf{x}, \mathbf{x}') dS'$

Electric scalar potential       $\Phi(\mathbf{x}) = \frac{j}{\epsilon\omega} \int_{S'} \nabla' \cdot \mathbf{J}(\mathbf{x}') G(\mathbf{x}, \mathbf{x}') dS'$

Electric vector potential       $\mathbf{F}(\mathbf{x}) = \epsilon \int_{S'} \mathbf{M}(\mathbf{x}') G(\mathbf{x}, \mathbf{x}') dS'$

Green's function       $G(\mathbf{x}, \mathbf{x}') = \frac{e^{-jkR}}{4\pi R}, \quad R = |\mathbf{x} - \mathbf{x}'|$

Singularity when  $R \rightarrow 0$

$\mathbf{J}$  and  $\mathbf{M}$  are electric and magnetic surface current densities

$S' = S$  is surface of scatterer

$\mu$  and  $\epsilon$  are permeability and permittivity of surrounding medium

$k = \omega\sqrt{\mu\epsilon}$  is wavenumber

# The Electric-Field Integral Equation (continued)

Compute  $\mathbf{J}$  and  $\mathbf{M}$  from incident electric field  $\mathbf{E}^I$

Discretize surface with triangles, approximate  $\mathbf{J}$  with RWG basis functions:

$$\mathbf{J}_h(\mathbf{x}) = \sum_{j=1}^{n_b} J_j \boldsymbol{\Lambda}_j(\mathbf{x})$$

Project EFIE onto vector-valued RWG basis functions

Express  $\mathbf{M}$  in terms of filament magnetic current  $\mathbf{I}_m$

Discretize wire with bars, approximate  $\mathbf{I}_m$  with 1D basis functions:

$$\mathbf{I}_h(s) = \sum_{j=1}^{n_b^m} I_j \boldsymbol{\Lambda}_j^m(s)$$

# The Slot Equation

The magnetic current along the slot is modeled using transmission line theory:

$$\mathbf{s} \cdot \left[ \mathbf{J} \times \mathbf{n} + \frac{1}{4} \left( Y_L \frac{d^2}{ds^2} - Y_C \right) \mathbf{I}_m \right] = 0$$

$$\mathbf{I}_m(0) = \mathbf{I}_m(L) = \mathbf{0}$$

$\mathbf{s}$  is the direction of the wire

Effective wire radius  $a$  obtained from conformal mapping using  $w$  and  $d$

$Y_L$  and  $Y_C$  are transmission line parameters (depend on  $w$ ,  $d$ , and materials)

Project slot equation onto vector-valued 1D basis functions

## Discretized Problem

Find  $\mathbf{J}_h \in \mathbb{V}_h$  and  $\mathbf{I}_h \in \mathbb{V}_h^m$ , such that

$$a_{\mathcal{E},\mathcal{E}}(\mathbf{J}_h, \boldsymbol{\Lambda}_i) + a_{\mathcal{E},\mathcal{M}}(\mathbf{I}_h, \boldsymbol{\Lambda}_i) = b_{\mathcal{E}}(\mathbf{E}^{\mathcal{I}}, \boldsymbol{\Lambda}_i) \quad \text{for } i = 1, \dots, n_b \quad (\text{EFIE})$$

$$a_{\mathcal{M},\mathcal{E}}(\mathbf{J}_h, \boldsymbol{\Lambda}_i^m) + a_{\mathcal{M},\mathcal{M}}(\mathbf{I}_h, \boldsymbol{\Lambda}_i^m) = 0 \quad \text{for } i = 1, \dots, n_b^m \quad (\text{Slot})$$

Evaluate EFIE on exterior and interior surfaces:  $n_b^{\text{ext}} + n_b^{\text{int}}$  unknowns for  $\mathbf{J}_h$

For thick slot,  $\mathbf{I}_m^{\text{ext}} = -\mathbf{I}_m^{\text{int}}$ :  $n_b^m$  unknowns for  $\mathbf{I}_h$

# Matrix–Vector Form

In matrix–vector form, solve for  $\mathcal{J}^h$ :

$$\mathbf{Z}\mathcal{J}^h = \mathbf{V}$$

$$\mathbf{Z} = \begin{bmatrix} \mathbf{A}^{\text{ext}} & \mathbf{0} & \mathbf{B}^{\text{ext}} \\ \mathbf{0} & \mathbf{A}^{\text{int}} & -\mathbf{B}^{\text{int}} \\ \mathbf{C}^{\text{ext}} & -\mathbf{C}^{\text{int}} & \mathbf{D} \end{bmatrix}, \quad \mathcal{J}^h = \begin{Bmatrix} \mathbf{J}^{h\text{ext}} \\ \mathbf{J}^{h\text{int}} \\ \mathbf{I}^h \end{Bmatrix}, \quad \mathbf{V} = \begin{Bmatrix} \mathbf{V}^{\mathcal{E}\text{ext}} \\ \mathbf{V}^{\mathcal{E}\text{int}} \\ \mathbf{0} \end{Bmatrix},$$

Impedance matrix                      Current vector                      Excitation vector

where

$$A_{i,j} = a_{\mathcal{E},\mathcal{E}}(\Lambda_j, \Lambda_i), \quad B_{i,j} = a_{\mathcal{E},\mathcal{M}}(\Lambda_j^m, \Lambda_i), \quad C_{i,j} = a_{\mathcal{M},\mathcal{E}}(\Lambda_j, \Lambda_i^m), \quad D_{i,j} = 2a_{\mathcal{M},\mathcal{M}}(\Lambda_j^m, \Lambda_i^m),$$

$$J_j^h = J_j, \quad I_j^h = I_j, \quad V_j^{\mathcal{E}} = b_{\mathcal{E}}(\mathbf{E}^{\mathcal{I}}, \Lambda_i)$$

More compactly:

$$\mathbf{Z} = \begin{bmatrix} \mathbf{A} & \mathbf{B} \\ \mathbf{C} & \mathbf{D} \end{bmatrix}, \quad \mathcal{J}^h = \begin{Bmatrix} \mathbf{J}^h \\ \mathbf{I}^h \end{Bmatrix}, \quad \mathbf{V} = \begin{Bmatrix} \mathbf{V}^{\mathcal{E}} \\ \mathbf{0} \end{Bmatrix}$$

# Outline

- Introduction
- Governing Equations
- Code-Verification Approaches
  - Manufactured Solutions
  - Solution-Discretization Error
  - Numerical-Integration Error
  - Manufactured Green's Function
- Numerical Examples
- Summary

# Manufactured Solutions for the EFIE

Continuous:  $r_{\mathcal{E}_i}(\mathbf{J}, \mathbf{I}_m) = a_{\mathcal{E}, \mathcal{E}}(\mathbf{J}, \boldsymbol{\Lambda}_i) + a_{\mathcal{E}, \mathcal{M}}(\mathbf{I}_m, \boldsymbol{\Lambda}_i) - b_{\mathcal{E}}(\mathbf{E}^{\mathcal{I}}, \boldsymbol{\Lambda}_i) = 0$

Discretized:  $r_{\mathcal{E}_i}(\mathbf{J}_h, \mathbf{I}_h) = a_{\mathcal{E}, \mathcal{E}}(\mathbf{J}_h, \boldsymbol{\Lambda}_i) + a_{\mathcal{E}, \mathcal{M}}(\mathbf{I}_h, \boldsymbol{\Lambda}_i) - b_{\mathcal{E}}(\mathbf{E}^{\mathcal{I}}, \boldsymbol{\Lambda}_i) = 0$

Method of manufactured solutions modifies discretized equations:

$$\mathbf{r}_{\mathcal{E}}(\mathbf{J}_h, \mathbf{I}_h) = \mathbf{r}_{\mathcal{E}}(\mathbf{J}_{MS}, \mathbf{I}_{MS})$$

$\mathbf{J}_{MS}$  and  $\mathbf{I}_{MS}$  are manufactured solutions,  $\mathbf{r}_{\mathcal{E}}(\mathbf{J}_{MS}, \mathbf{I}_{MS})$  is computed exactly

New Discretized:  $a_{\mathcal{E}, \mathcal{E}}(\mathbf{J}_h, \boldsymbol{\Lambda}_i) + a_{\mathcal{E}, \mathcal{M}}(\mathbf{I}_h, \boldsymbol{\Lambda}_i) = \underbrace{a_{\mathcal{E}, \mathcal{E}}(\mathbf{J}_{MS}, \boldsymbol{\Lambda}_i) + a_{\mathcal{E}, \mathcal{M}}(\mathbf{I}_{MS}, \boldsymbol{\Lambda}_i)}_{= b_{\mathcal{E}}(\mathbf{E}^{\mathcal{I}}, \boldsymbol{\Lambda}_i)}: \text{implement via } \mathbf{E}^{\mathcal{I}}$

$$\begin{aligned} \mathbf{E}^{\mathcal{I}}(\mathbf{x}) &= \frac{j}{\epsilon\omega} \int_{S'} [k^2 \mathbf{J}_{MS}(\mathbf{x}') \mathbf{G}(\mathbf{x}, \mathbf{x}') + \nabla' \cdot \mathbf{J}_{MS}(\mathbf{x}') \nabla \mathbf{G}(\mathbf{x}, \mathbf{x}')] dS' + Z_s \mathbf{J}_{MS}(\mathbf{x}) \\ &\quad - \frac{1}{4} (\mathbf{n}(\mathbf{x}) \times \mathbf{I}_{MS}(\mathbf{x})) \delta_{slot}(\mathbf{x}) + \frac{1}{4\pi} \int_0^L \mathbf{I}_{MS}(s') \times \int_0^{2\pi} \nabla' \mathbf{G}(\mathbf{x}, \mathbf{x}') d\phi' ds' \end{aligned}$$

MMS incorporated through  $\mathbf{E}^{\mathcal{I}}$  – no additional source term required

# Manufactured Solutions for the Slot Equation

Continuous:  $r_{\mathcal{M}_i}(\mathbf{J}_m, \mathbf{I}_m) = a_{\mathcal{M}, \mathcal{E}}(\mathbf{J}_m, \boldsymbol{\Lambda}_i^m) + a_{\mathcal{M}, \mathcal{M}}(\mathbf{I}_m, \boldsymbol{\Lambda}_i^m) = 0$

Discretized:  $r_{\mathcal{M}_i}(\mathbf{J}_h, \mathbf{I}_h) = a_{\mathcal{M}, \mathcal{E}}(\mathbf{J}_h, \boldsymbol{\Lambda}_i^m) + a_{\mathcal{M}, \mathcal{M}}(\mathbf{I}_h, \boldsymbol{\Lambda}_i^m) = 0$

Method of manufactured solutions modifies discretized equations:

$$\mathbf{r}_{\mathcal{M}}(\mathbf{J}_h, \mathbf{I}_h) = \mathbf{r}_{\mathcal{M}}(\mathbf{J}_{MS}, \mathbf{I}_{MS})$$

New Discretized:

$$a_{\mathcal{M}, \mathcal{E}}(\mathbf{J}_h, \boldsymbol{\Lambda}_i^m) + a_{\mathcal{M}, \mathcal{M}}(\mathbf{I}_h, \boldsymbol{\Lambda}_i^m) = \underbrace{a_{\mathcal{M}, \mathcal{E}}(\mathbf{J}_{MS}, \boldsymbol{\Lambda}_i^m) + a_{\mathcal{M}, \mathcal{M}}(\mathbf{I}_{MS}, \boldsymbol{\Lambda}_i^m)}_{= 0: \text{ no source term needed}}$$

Given  $\mathbf{J}_{MS}$ , solve for  $\mathbf{I}_{MS}$  to avoid source term

## Solution-Discretization Error

- Error due to basis-function approximations of solutions:

$$\mathbf{J}_h(\mathbf{x}) = \sum_{j=1}^{n_b} J_j \boldsymbol{\Lambda}_j(\mathbf{x}), \quad \mathbf{I}_h(s) = \sum_{j=1}^{n_b^m} I_j \boldsymbol{\Lambda}_j^m(s)$$

- Measured with discretization errors:  $\mathbf{e}_{\mathbf{J}} = \mathbf{J}^h - \mathbf{J}_n, \quad \mathbf{e}_{\mathbf{I}} = \mathbf{I}^h - \mathbf{I}_s$

$$\|\mathbf{e}_{\mathbf{J}}\| \leq C_{\mathbf{J}} h^{p_{\mathbf{J}}}, \quad \|\mathbf{e}_{\mathbf{I}}\| \leq C_{\mathbf{I}} h^{p_{\mathbf{I}}}$$

$J_{n_j}$ : component of  $\mathbf{J}_{MS}$  flowing from  $T_j^+$  to  $T_j^-$

$I_{s_j}$ : component of  $\mathbf{I}_{MS}$  flowing along  $\mathbf{s}$  at  $s_j$

$C$ : function of solution derivatives

$h$ : measure of mesh size

$p$ : order of accuracy

- Compute  $p$  from  $\|\mathbf{e}\|$  across multiple meshes (expect  $p = 2$  for these bases)
- Avoid numerical-integration error if integrating exactly

# Solution-Discretization Error: Discontinuity

- $\delta_{\text{slot}}$  introduces discontinuity due to wire interaction with surface
- Discontinuity impacts  $\mathbf{E}^{\mathcal{I}}$  for MMS
- Discontinuity will contaminate convergence studies:  $\mathcal{O}(h^2) \rightarrow \mathcal{O}(h)$
- Discontinuity denoted by  $\mathbf{B}_1$  in  $\mathbf{Z} = \begin{bmatrix} \mathbf{A} & (\mathbf{B}_1 + \mathbf{B}_2) \\ \mathbf{C} & \mathbf{D} \end{bmatrix}$
- Since  $\mathbf{B}_1 = -\frac{1}{4}\mathbf{C}^T$ , use  $\mathbf{C}$  to cancel contribution from  $\mathbf{B}_1$  and modify  $\mathbf{E}^{\mathcal{I}}$ :

$$\mathbf{Z} = \begin{bmatrix} \mathbf{A} & (\cancel{\mathbf{B}_1} + \mathbf{B}_2) \\ \mathbf{C} & \mathbf{D} \end{bmatrix},$$

$$\mathbf{E}^{\mathcal{I}} = \frac{j}{\epsilon\omega} \int_{S'} [k^2 \mathbf{J}_{\text{MS}} G + \nabla' \cdot \mathbf{J}_{\text{MS}} \nabla G] dS' - \cancel{\frac{1}{4}(\mathbf{n} \times \mathbf{I}_{\text{MS}}) \delta_{\text{slot}}} + \frac{1}{4\pi} \int_0^L \mathbf{I}_{\text{MS}} \times \int_0^{2\pi} \nabla' G d\phi' ds' + Z_s \mathbf{J}_{\text{MS}}$$

- Correctness of  $\mathbf{B}_1$  is assessed by successful removal using  $\mathbf{C}$
- Correctness of  $\mathbf{C}$  is assessed through the mesh-convergence study

# Numerical-Integration Error

- Error due to quadrature integral evaluation  $(\cdot)^q$  on both sides of equations
- Measure numerical-integration error:

$$e_a = \mathcal{J}^H(\mathbf{Z}^q - \mathbf{Z})\mathcal{J}, \quad e_b = \mathcal{J}^H(\mathbf{V}^q - \mathbf{V}),$$

where  $\mathcal{J} = \begin{Bmatrix} \mathbf{J}_n \\ \mathbf{I}_s \end{Bmatrix}$

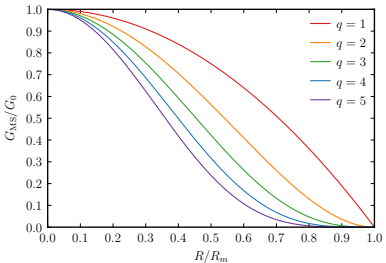
- Solution-discretization error is canceled
- $|e_a| \leq C_a h^{p_a}$  and  $|e_b| \leq C_b h^{p_b}$ 
  - $C$ : function of integrand derivatives
  - $p$ : order of accuracy of quadrature rules
- With multiple meshes, compute  $p$  from  $|e|$

# Manufactured Green's Function

Integrals with  $G$  cannot be computed analytically or, when  $R \rightarrow 0$ , accurately

Inaccurately computing integrals on either side contaminates convergence studies

Manufacture Green's function:  $G_{\text{MS}}(R) = G_0 \left(1 - \frac{R^2}{R_m^2}\right)^q$ ,  $R_m = \max_{\mathbf{x}, \mathbf{x}' \in S} R$  and  $q \in \mathbb{N}$



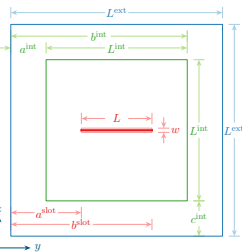
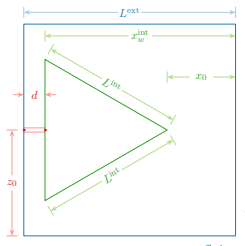
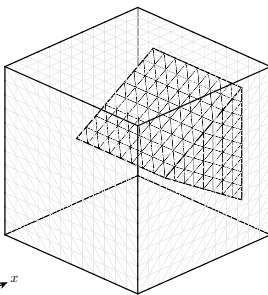
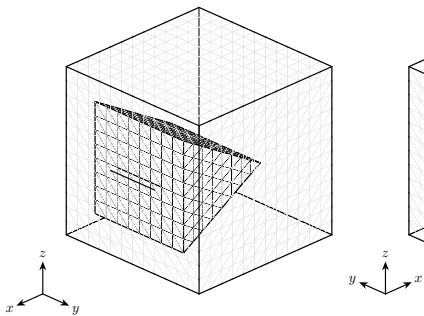
Reasoning:

- 1) Even powers of  $R$  permit integrals to be computed analytically
- 2)  $G_{\text{MS}}$  increases when  $R$  decreases, as with actual  $G$

# Outline

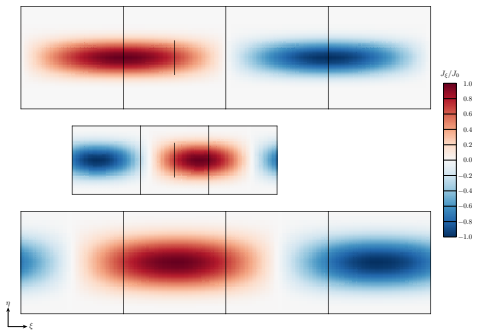
- Introduction
- Governing Equations
- Code-Verification Approaches
- Numerical Examples
  - Overview
  - Solution-Discretization Error
  - Numerical-Integration Error
- Summary

## Cubic Scatterer with a Triangularly Prismatic Cavity

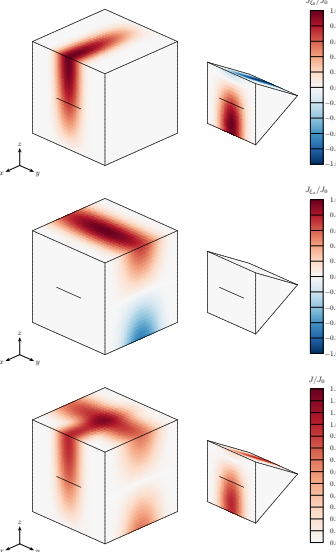


- $L^{\text{ext}} = 1 \text{ m}$ ,  $L^{\text{int}} = 2L^{\text{ext}}/3$ ,  $L = L^{\text{ext}}/3$ ,  $w = L^{\text{ext}}/50$
  - $a^{\text{int}} = L^{\text{ext}}/6$ ,  $c^{\text{int}} = L^{\text{ext}}/6$ ,  $z_0 = L^{\text{ext}}/2$
  - $\mu = \mu_0$ ,  $\epsilon = \epsilon_0$ ,  $k = 2\pi \text{ m}^{-1}$ ,  $\sigma$  of aluminum
  - 3 depths:  $d_1 = L^{\text{ext}}/10$ ,  $d_2 = L^{\text{ext}}/100$ ,  $d_3 = L^{\text{ext}}/1000$
  - 2 Green's functions:  $G_1$ ,  $G_2$

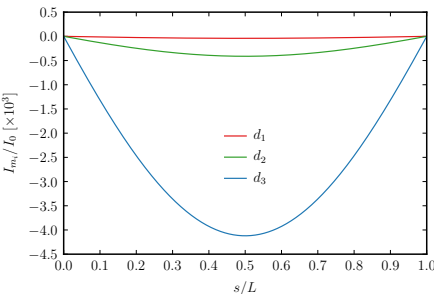
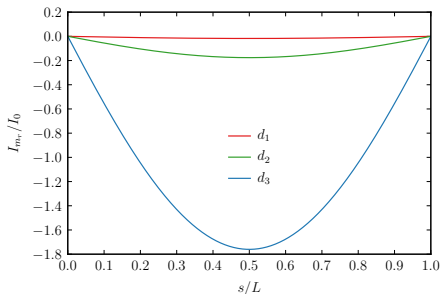
# Manufactured Solutions



- Manufacture solutions for 2D strips of class  $C^2$
- Wrap strips around lateral surfaces of prisms
- Solutions are product of  $\xi$  and  $\eta$  dependencies
  - $\xi$  dependency: sinusoid with a single period
  - $\eta$  dependency: cubed sinusoid with a half period
- Current flows along  $\xi$ ; at slot,  $J_\xi^{\text{ext}} = J_\xi^{\text{int}}$



# Magnetic Current



- Instead of arbitrarily manufacturing  $\mathbf{I}_{\text{MS}} = I_m \mathbf{s}$ , solve for it given  $\mathbf{J}_{\text{MS}}$ :

$$-J_{\xi_\theta}(\boldsymbol{\xi}) + \frac{1}{4} \left( Y_L \frac{d^2}{ds^2} - Y_C \right) I_m(s) = 0$$

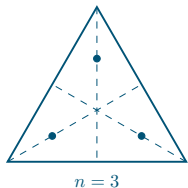
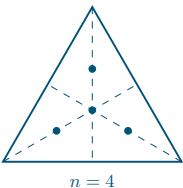
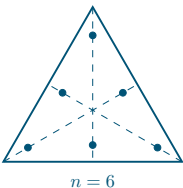
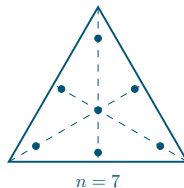
- Solution is

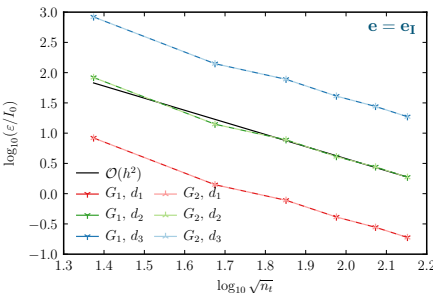
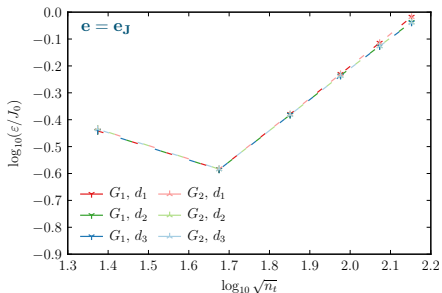
$$I_m(s) = C_1 \cosh\left(\frac{s}{Z}\right) + C_2 \sinh\left(\frac{s}{Z}\right) + C_3 \sin\left(\frac{\pi(s + \Delta a)}{L^{\text{int}}}\right) + C_4 \cos\left(\frac{\pi(s + \Delta a)}{L^{\text{int}}}\right)$$

# Numerical Integration

- Surface integrals evaluated using 2D triangle quadrature rules
- Wire integrals evaluated using 1D bar quadrature rules

Maximum integrand degree	Number of 2D points	Number of 1D points	Convergence rate
1	1	1	$\mathcal{O}(h^2)$
2	3	—	$\mathcal{O}(h^4)$
3	4	2	$\mathcal{O}(h^4)$
4	6	—	$\mathcal{O}(h^6)$
5	7	3	$\mathcal{O}(h^6)$

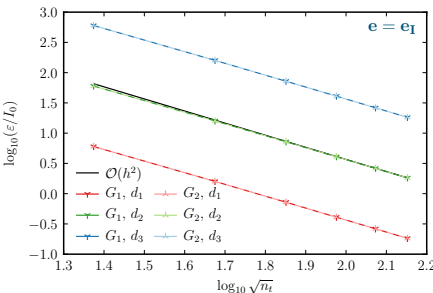
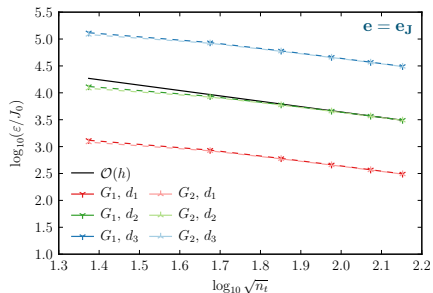
 $n = 3$  $n = 4$  $n = 6$  $n = 7$

Solution-Discretization Error:  $\varepsilon = \|\mathbf{e}\|_\infty (\mathbf{e}_J \leftrightarrow \mathbf{e}_I)$ 

- Discontinuity present:

$$\begin{bmatrix} \mathbf{A} & \mathbf{B} \\ \mathbf{C} & \mathbf{D} \end{bmatrix} \begin{Bmatrix} \mathbf{J}^h \\ \mathbf{I}^h \end{Bmatrix} = \begin{Bmatrix} \mathbf{V}^\varepsilon \\ \mathbf{0} \end{Bmatrix}$$

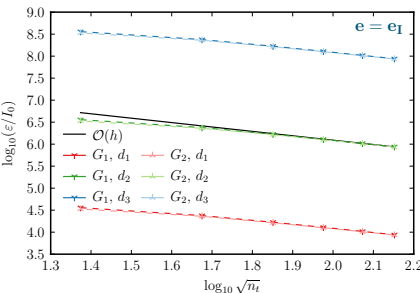
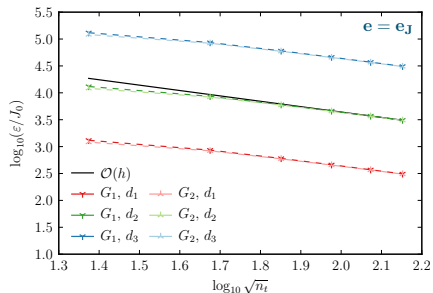
- $\mathbf{e}_J$  and  $\mathbf{e}_I$  are interdependent ( $\mathbf{e}_J \leftrightarrow \mathbf{e}_I$ )
- Convergence rate for  $\|\mathbf{e}_J\|_\infty$  is negative – not exhibiting asymptotic convergence
- Convergence rate for  $\|\mathbf{e}_I\|_\infty$  is close to  $\mathcal{O}(h^2)$

Solution-Discretization Error:  $\varepsilon = \|\mathbf{e}\|_\infty$  ( $\mathbf{e}_J \leftrightarrow \mathbf{e}_I$ )

- Decouple discretization errors:

$$\begin{bmatrix} \mathbf{A} & \mathbf{B} \\ \mathbf{C} & \mathbf{D} \end{bmatrix} \begin{Bmatrix} \mathbf{J}^h \\ \mathbf{I}^h \end{Bmatrix} = \begin{Bmatrix} \mathbf{V}^\varepsilon \\ \mathbf{0} \end{Bmatrix} \rightarrow \begin{bmatrix} \mathbf{A} & \mathbf{0} \\ \mathbf{0} & \mathbf{D} \end{bmatrix} \begin{Bmatrix} \mathbf{J}^h \\ \mathbf{I}^h \end{Bmatrix} = \begin{Bmatrix} \mathbf{V}^\varepsilon - \mathbf{BI}_s \\ -\mathbf{CJ}_n \end{Bmatrix}$$

- $\mathbf{e}_J$  and  $\mathbf{e}_I$  are independent ( $\mathbf{e}_J \leftrightarrow \mathbf{e}_I$ )
- Convergence rates for  $\|\mathbf{e}_J\|_\infty$  and  $\|\mathbf{e}_I\|_\infty$  are  $\mathcal{O}(h)$  and  $\mathcal{O}(h^2)$  as expected
- $\|\mathbf{e}_J\|_\infty$  is much larger than when  $\mathbf{e}_J \leftrightarrow \mathbf{e}_I$

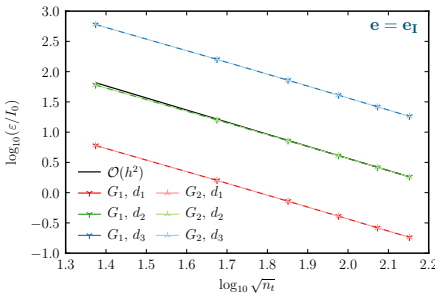
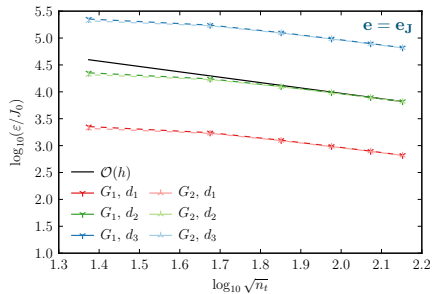
Solution-Discretization Error:  $\varepsilon = \|\mathbf{e}\|_\infty$  ( $\mathbf{e}_J \rightarrow \mathbf{e}_I$ )

- Remove influence of  $\mathbf{e}_I$  on  $\mathbf{e}_J$ , preserve influence of  $\mathbf{e}_J$  on  $\mathbf{e}_I$ :

$$\begin{bmatrix} \mathbf{A} & \mathbf{B} \\ \mathbf{C} & \mathbf{D} \end{bmatrix} \begin{Bmatrix} \mathbf{J}^h \\ \mathbf{I}^h \end{Bmatrix} = \begin{Bmatrix} \mathbf{V}^\varepsilon \\ \mathbf{0} \end{Bmatrix} \rightarrow \begin{bmatrix} \mathbf{A} & \mathbf{0} \\ \mathbf{C} & \mathbf{D} \end{bmatrix} \begin{Bmatrix} \mathbf{J}^h \\ \mathbf{I}^h \end{Bmatrix} = \begin{Bmatrix} \mathbf{V}^\varepsilon - \mathbf{BI}_s \\ \mathbf{0} \end{Bmatrix}$$

- $\mathbf{e}_J$  affects  $\mathbf{e}_I$  ( $\mathbf{e}_J \rightarrow \mathbf{e}_I$ )
- Convergence rates for  $\|\mathbf{e}_J\|_\infty$  and  $\|\mathbf{e}_I\|_\infty$  are  $\mathcal{O}(h)$  as expected
- $\|\mathbf{e}_J\|_\infty$  and  $\|\mathbf{e}_I\|_\infty$  are much larger than when  $\mathbf{e}_J \leftrightarrow \mathbf{e}_I$

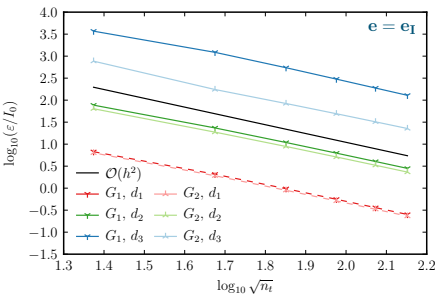
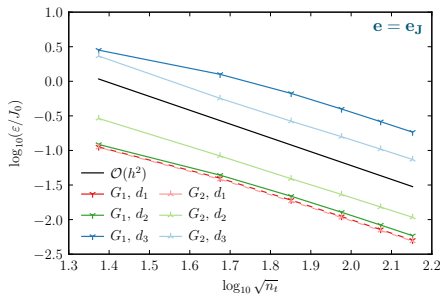
# Solution-Discretization Error: $\varepsilon = \|\mathbf{e}\|_\infty$ ( $\mathbf{e}_J \leftarrow \mathbf{e}_I$ )



- Remove influence of  $\mathbf{e}_J$  on  $\mathbf{e}_I$ , preserve influence of  $\mathbf{e}_I$  on  $\mathbf{e}_J$ :

$$\begin{bmatrix} \mathbf{A} & \mathbf{B} \\ \mathbf{C} & \mathbf{D} \end{bmatrix} \begin{Bmatrix} \mathbf{J}^h \\ \mathbf{I}^h \end{Bmatrix} = \begin{Bmatrix} \mathbf{V}^\varepsilon \\ \mathbf{0} \end{Bmatrix} \rightarrow \begin{bmatrix} \mathbf{A} & \mathbf{B} \\ \mathbf{0} & \mathbf{D} \end{bmatrix} \begin{Bmatrix} \mathbf{J}^h \\ \mathbf{I}^h \end{Bmatrix} = \begin{Bmatrix} \mathbf{V}^\varepsilon \\ -\mathbf{CJ}_n \end{Bmatrix}$$

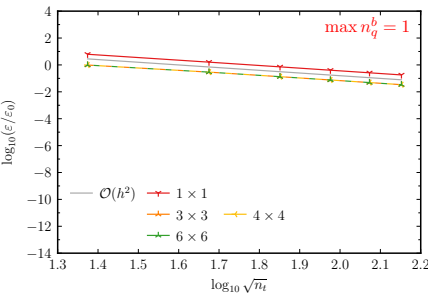
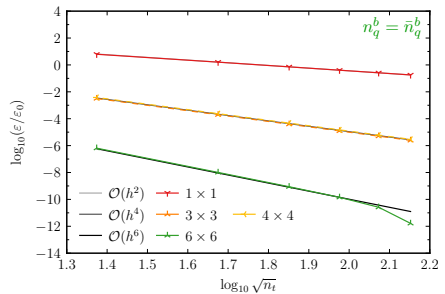
- $\mathbf{e}_I$  affects  $\mathbf{e}_J$  ( $\mathbf{e}_J \leftarrow \mathbf{e}_I$ )
- Convergence rates for  $\|\mathbf{e}_J\|_\infty$  and  $\|\mathbf{e}_I\|_\infty$  are  $\mathcal{O}(h)$  and  $\mathcal{O}(h^2)$  as expected
- $\|\mathbf{e}_J\|_\infty$  is much larger than when  $\mathbf{e}_J \leftrightarrow \mathbf{e}_I$

Solution-Discretization Error:  $\varepsilon = \|\mathbf{e}\|_\infty$  (Discontinuity Removed)

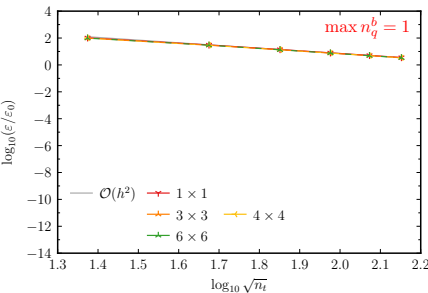
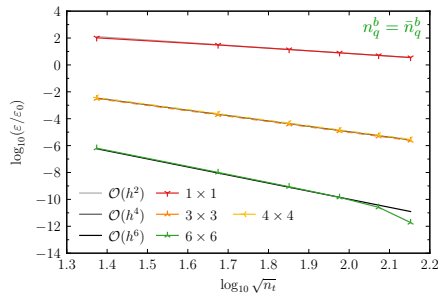
- Discontinuity removed from  $\mathbf{Z}$  using  $\mathbf{C}$ , corresponding MMS source term omitted in  $\mathbf{V}^\varepsilon$ :

$$\begin{bmatrix} \mathbf{A} & \mathbf{B} \\ \mathbf{C} & \mathbf{D} \end{bmatrix} \begin{Bmatrix} \mathbf{J}^h \\ \mathbf{I}^h \end{Bmatrix} = \begin{Bmatrix} \mathbf{V}^\varepsilon \\ \mathbf{0} \end{Bmatrix} \rightarrow \begin{bmatrix} \mathbf{A} & (\mathbf{B}_1 + \mathbf{B}_2) \\ \mathbf{C} & \mathbf{D} \end{bmatrix} \begin{Bmatrix} \mathbf{J}^h \\ \mathbf{I}^h \end{Bmatrix} = \begin{Bmatrix} \mathbf{V}^\varepsilon \\ \mathbf{0} \end{Bmatrix}$$

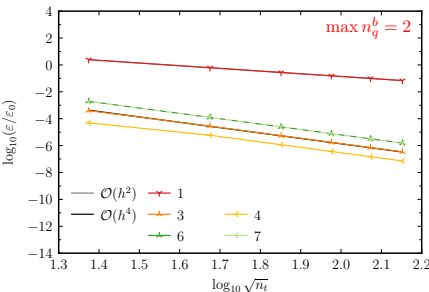
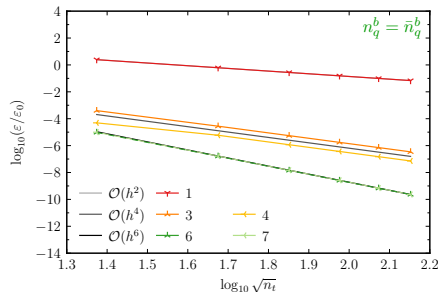
- Convergence rates for  $\|\mathbf{e}_J\|_\infty$  and  $\|\mathbf{e}_I\|_\infty$  are  $\mathcal{O}(h^2)$  as expected
- Correct implementation of  $\mathbf{B}_1$  suggested by its removal using  $\mathbf{C}$
- Correct implementation of  $\mathbf{C}$  suggested by expected convergence rates

Numerical-Integration Error:  $\varepsilon = |e_a|$  ( $G = G_2$ ,  $d = d_1$ )

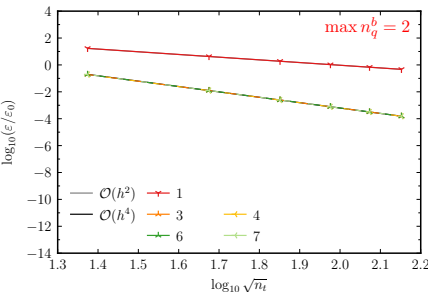
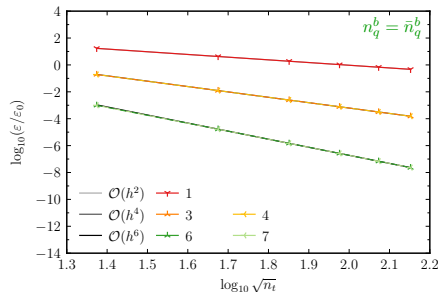
- 2D points: [number for test integral]  $\times$  [number for source integral]
- 1D points:  $\bar{n}_q^b$  = number of 1D points with same convergence rate as 2D points
- Convergence rates are as expected for  $n_q^b = \bar{n}_q^b$
- Convergence rates are limited to  $\mathcal{O}(h^2)$  for  $n_q^b = 1$

Numerical-Integration Error:  $\varepsilon = |e_a|$  ( $G = G_2$ ,  $d = d_3$ )

- 2D points: [number for test integral]  $\times$  [number for source integral]
- 1D points:  $\bar{n}_q^b$  = number of 1D points with same convergence rate as 2D points
- Convergence rates are as expected for  $n_q^b = \bar{n}_q^b$
- Convergence rates are limited to  $\mathcal{O}(h^2)$  for  $n_q^b = 1$

Numerical-Integration Error:  $\varepsilon = |e_b|$  ( $G = G_2$ ,  $d = d_1$ )

- 2D points: number for test integral
- 1D points:  $\bar{n}_q^b$  = number of 1D points with same convergence rate as 2D points
- Convergence rates are as expected for  $n_q^b = \bar{n}_q^b$
- Convergence rates are limited to  $\mathcal{O}(h^4)$  for  $n_q^b = 2$

Numerical-Integration Error:  $\varepsilon = |e_b|$  ( $G = G_2$ ,  $d = d_3$ )

- 2D points: number for test integral
- 1D points:  $\bar{n}_q^b$  = number of 1D points with same convergence rate as 2D points
- Convergence rates are as expected for  $n_q^b = \bar{n}_q^b$
- Convergence rates are limited to  $\mathcal{O}(h^4)$  for  $n_q^b = 2$

# Outline

- Introduction
- Governing Equations
- Code-Verification Approaches
- Numerical Examples
- Summary
  - Closing Remarks

## Closing Remarks

3 error sources in electromagnetic integral equations:

- **Domain-discretization error** – avoided
  - Considered planar surfaces
- **Solution-discretization error** – isolated
  - Manufactured  $\mathbf{J}$ , obtained  $\mathbf{I}_m$  without source term
  - Manufactured Green's function (to integrate exactly)
  - Removed discontinuity to measure convergence rates without contamination
  - Demonstrated discontinuity implications by varying  $\mathbf{e_J} \leftrightarrow \mathbf{e_I}$
- **Numerical-integration error** – isolated
  - Canceled basis-function contribution
  - Detected coding error

Achieved expected orders of accuracy

Questions?

[bafreno@sandia.gov](mailto:bafreno@sandia.gov)[brianfreno.github.io](https://brianfreno.github.io)

## Additional Information

- B. Freno, N. Matula, W. Johnson  
Manufactured solutions for the method-of-moments implementation of the EFIE  
*Journal of Computational Physics* (2021) [arXiv:2012.08681](https://arxiv.org/abs/2012.08681)
- B. Freno, N. Matula, J. Owen, W. Johnson  
Code-verification techniques for the method-of-moments implementation of the EFIE  
*Journal of Computational Physics* (2022) [arXiv:2106.13398](https://arxiv.org/abs/2106.13398)
- B. Freno, N. Matula  
Code verification for practically singular equations  
*Journal of Computational Physics* (2022) [arXiv:2204.01785](https://arxiv.org/abs/2204.01785)
- B. Freno, N. Matula  
Code-verification techniques for the method-of-moments implementation of the MFIE  
*Journal of Computational Physics* (2023) [arXiv:2209.09378](https://arxiv.org/abs/2209.09378)
- B. Freno, N. Matula  
Code-verification techniques for the method-of-moments implementation of the CFIE  
*Journal of Computational Physics* (2023) [arXiv:2302.06728](https://arxiv.org/abs/2302.06728)
- B. Freno, N. Matula, R. Pfeiffer, E. Dohme, J. Kotulski  
Manufactured solutions for an electromagnetic slot model  
[arXiv:2406.14573](https://arxiv.org/abs/2406.14573)

